Latin American Journal of Solids and Structures
www.lajss.org

Numerical Study on Steel Shear Walls with Sinusoidal Corrugated Plates

Abstract

Over the past decades a growing demand and interest has stimulated many researchers to investigate different aspects of steel plate shear walls (SPSWs). The structural performance of steel shear walls with sinusoidal corrugated plate infills is investigated in this study. Finite element (FE) analysis was adopted using ANSYS software, wherein flat and corrugatedshear walls – with different thicknesses, various corrugation numbers and angles – were modeled under monotonic and cyclic loads. Results and findings of this study indicate that geometrical variations developed through corrugation can be effective on the capacity, rigidity, and post-yielding responses of such corrugated-web lateral force-resisting systems. In addition, proper design and detailing can result in desirable structural behavior and seismic performance of SPSWs with sinusoidal corrugated infill plates.

Keywords

Steel plate shear walls, Sinusoidal corrugated plates, Numerical simulation, Structural performance.

Hamed Kalali [a]
Tohid Ghanbari Ghazijahani [b]
Mohammad Hajsadeghi [c]
Tadeh Zirakian [d,*]
Farshid J. Alaee [a]

[a] Department of Civil Engineering and Architecture, University of Shahrood, Shahrood, Iran
[b] School of Engineering& ICT, University of Tasmania, Hobart, Australia
[c] School of Engineering Sciences, University of Liverpool, Liverpool L69 3BX, UK
[d] Department of Civil Engineering and Construction Management, California State University, Northridge, CA, USA

[*] Corresponding Author; Phone: +1-818-677-7718, Fax: +1-818-677-5810, E-mail: tadeh.zirakian@csun.edu

http://dx.doi.org/10.1590/1679-78252837

Received 02.05.2016
In revised form 31.07.2016
Accepted 31.08.2016
Available online 03.09.2016

1 INTRODUCTION

Steel plate shear walls (SPSWs) are widely used in construction industry due to their salient features of cost-effectiveness, great ductility and feasibility of construction. Cold formed steel wall

frames are employed – especially in low and mid-rise buildings – alongside the plate infill to resist and dissipate the seismic energy through lateral plastic deformations. Many researchers have been motivated by the topic and accordingly set forth the structural response of steel shear walls under static and seismic loadings. In the most recent investigations, Wang and Ye (2015), Purba and Bruneau (2015), Mohebbi et al. (2015), Sabouri-Ghomi and Mamazizi (2015), Zirakian and Zhang (2015), and Zhang and Zirakian (2015) provided input into different aspects of steel shear walls. In these studies, the effect of geometry on the strength, energy dissipation and rigidity of such structures were thoroughly expounded upon respectively.

Corrugated steel shear walls, albeit to a lesser extent, have been reflected upon in the literature as well as the plain shear walls. Tipping and a few collaborators, i.e. Stojadinovic and Tipping (2007) and Vigh et al. (2014), experimentally studied corrugated shear walls subject to cyclic lateral loading. A standard model, applicable to different shear walls, was proposed and genetic algorithm was employed and optimized in this study to reach cyclic deterioration parameters. Vora and Yu (2008), also, conducted monotonic and cyclic tests on corrugated shear walls. It was found that appropriate framing elements along with proper fastener configurations can lead to a reliable rigid sheathing provided by corrugated steel plates. The behavior of trapezoidal corrugated steel plate shear walls was examined by Farzampour and Laman (2015). It appeared that although the ultimate capacity of such shear walls may result in a reduction of the ductility, initial lateral stiffness and energy absorption increase if the trapezoidal walls are utilized as plate infills. Cyclic behavior of trapezoidal shear walls was investigated by Emami et al. (2013). Notwithstanding good correlations between the experiments and the analytical studies, further works into trapezoidal shear walls were proposed by the authors of this paper so as to elucidate further aspects of such structures.

Full-scale shear corrugated sheets with and without wall panels were investigated by Fülöp and Dubina (2004a). This study was followed by a counterpart numerical modeling on the earthquake performance of the mentioned experimental specimens (Fülöp and Dubina, 2004b). The two mentioned investigations yielded proper comparisons between experiments and FE results. Seismic performance of corrugated steel shear walls was undertaken by Vigh et al. (2013) through a nonlinear analysis. In this study, appropriate seismic performance factors were proposed by the researchers. Elastic buckling of steel shear walls corrugated in trapezoidal shapes was looked into by Tong and Guo (2015). A number of formulas, to obtain elastic buckling coefficients, were proposed for stiffened models through this study. Steel sheathed cold-formed trussed shear walls (SSCFSTSWs) with a corrugated infill of different sheathing, skeleton configurations and chord studs were experimentally investigated by Tian et al. (2015). It was obtained that SSCFSTSWs brought about a greatly higher ultimate capacity than its conventional counterparts.

Despite copious papers in the literature on the structural performance of steel shear walls, it is believed that corrugated steel shear walls still need further detailed considerations. It is fitting to mention that the aforementioned studies on the corrugated shear walls were all performed experimentally. This requires the assessment of numerical studies to identify the reliability of FE analysis to evaluate the structural response of such corrugated plates. To this end, this paper aims at studying such structures by a FE modeling, wherein different geometric variables were applied to different models. These variations yielded different structural responses leading to significant insight into the performance of such elements under lateral cyclic loading.

2 NUMERICAL MODELING

2.1 Geometric Specifications of SPSW Models

Models in this study consisted of two main groups comprising flat and corrugated SPSWs. Geometric features of different models are listed in Table 1. Six flat plates alongside 16 corrugated plates were created and analyzed in this study. Two types of labels as F-T and C-ϑ-N-T were adopted, wherein F and C identify flat and corrugated plates, T stands for the thickness of the plates, and ϑ and N are the angle and the number of corrugations, respectively. Overall view of the geometry of corrugated and plain walls are seen in Figures 1 and 2. Both flat and corrugated shear walls were encompassed with two beams and columns configured as a single span single story frame such that the frame was adequately restrained to avoid any out-of-plane displacements and local plastic deformations. As shown in Figure 1, 134×75×8 mm stiffeners were placed on both sides and at four corners of the frame literally at the upper and lower ends of the panel zones. Additionally, 116×65×8 mm stiffeners were placed at various locations and on both sides of the upper HEB 140 boundary member. Figure 3 illustrates the sectional and perspective views of one SPSW model together with its meshing layout.

Thickness	$T = 1.25$ mm	$T = 2$ mm	$T = 3$ mm	$T = 4$ mm	$T = 5$ mm	$T = 6$ mm
Flat *(label: F-T)*	*F*-1.25	*F*-2	*F*-3	*F*-4	*F*-5	*F*-6
Corrugated *(label: C-ϑ-N-T)*	*C*-30-8-1.25	*C*-30-8-2	*C*-30-8-3 *C*-45-8-3 *C*-45-6-3 *C*-45-10-3 *C*-60-8-3 *C*-90-8-3	*C*-30-8-4	*C*-30-8-5	*C*-30-8-6 *C*-45-6-6 *C*-45-8-6 *C*-45-10-6 *C*-60-8-6 *C*-90-8-6

Note: F = Flat plate, C = Curved plate, T = Wall thickness, ϑ = Corrugation angle, and N = Number of corrugation half-waves.

Table 1: Properties of the considered models.

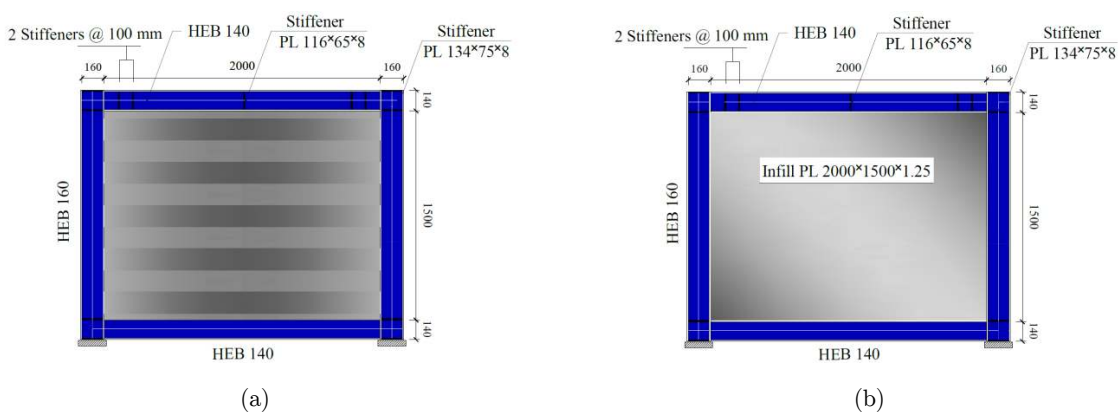

Figure 1: Overall view of corrugated and plain models.

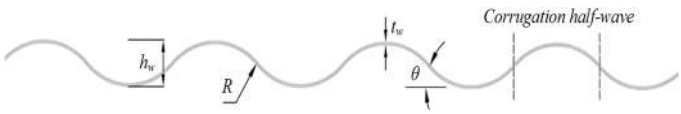

Figure 2: Geometry of the corrugations.

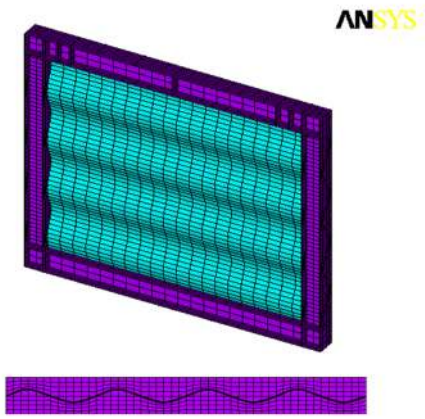

Figure 3: FE model and meshing layout of the numerical model *C*-30-8-1.25.

2.2 Modeling of SPSWs

ANSYS 11.0 (2007) as a finite element package was utilized in this study. Flat and sinusoidal corrugated shear walls were simulated using monotonic static loading buckling analysis, and cyclic loading as well. Mesh convergence study was carried out for the present models to determine as to what density of mesh is appropriate to gain converged load capacities. Eight-node SHELL93 element was employed for beam and column members of the frame as well as the plate walls. It is noteworthy that the utilized elements are capable of being used in models with large displacement and large strain values and are well suited to the plasticity and stress stiffening. Geometric and material nonlinearities were applied to the models.

2.3 Material Properties

Figure 4 shows the stress-strain response of the present models. As can be seen, beams, columns and the plates were simulated by three different material properties with different yield and ultimate stresses. The yield stresses of the beams, columns and plates were 288 MPa, 300 MPa and 207 MPa, respectively. The material input was defined according to three different stages in stress-strain curve representing yield, nonlinear stage and plastic region of the material. The Young's modulus and Poisson's ratio were taken as 200 GPa and 0.3, respectively, for all three materials.

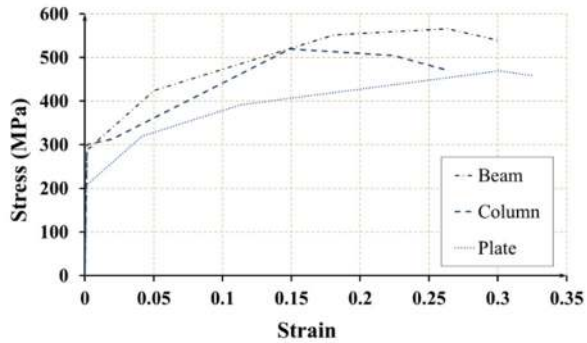

Figure 4: Material properties of beams, columns and plates.

2.4 Boundary Conditions

Boundary condition was modeled as clamped such that the plate infill in a model was fully restrained by the surrounding beam and column elements. Furthermore, out-of-plane displacements of the frame were restrained. For proper performance of the system, beam-to-column connections in the SPSW models were strengthened by using stiffeners at the top and bottom of the panel zones.

2.5 Loading Protocol

Lateral in-plane shear loading was applied to the top beam-column junction of the frames. Figure 5 shows the loading protocol, wherein γ and γ_y are rotation and yield rotationof the system, respectively. Rotation is considered as the ratio of the lateral displacement measured at the mid-height and mid-length of the top beam to height of the system measured between the beams centerlines. The cyclic loading comprised two force-controlled and displacement-controlled stages; in the first cycle, the load was applied in a force-controlled manner, while in the rest of the cycles, the load was applied in a displacement-controlled manner. It is noted that the steps used for displacement loading ranged from 10 to 16 for every 1 mm displacement.

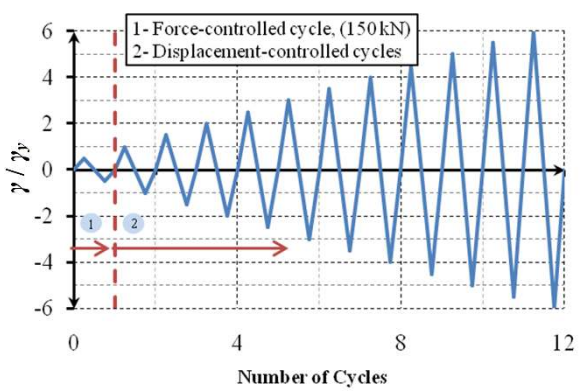

Figure 5: Loading protocol: number of cycles versus γ / γ_y.

3 VALIDATION OF NUMERICAL SIMULATIONS

The results of the present numerical simulations agreed well with the experimental results reported by Emami et al. (2013).In fact, the finite element simulations closely modeledthe tested specimens with flat and trapezoidally-corrugated webs, i.e. F-1.25 and T-30-8-1.25.The bar charts of Figure 6 show the consistence of the experimental results and the current FE modeling in ultimate strengths and displacements for two plain and corrugated models. For plain models, the discrepancies were less than 6% while the difference for the corrugated models was always less than 16%. By the same token, load-displacement response of the modeled corrugated SPSWs well agreed with the curves of the aforementioned experimental work (Figure 7).In spite of the inevitable limitations in modeling of the geometrical and material properties of the test specimens, the agreement between the experimental results and theoretical predictions is quite satisfactory. Accordingly, the current numerical analysis demonstrates the capability of the FE modeling in reliably predicting the structural strength of the corrugated models as well as the failure modes.

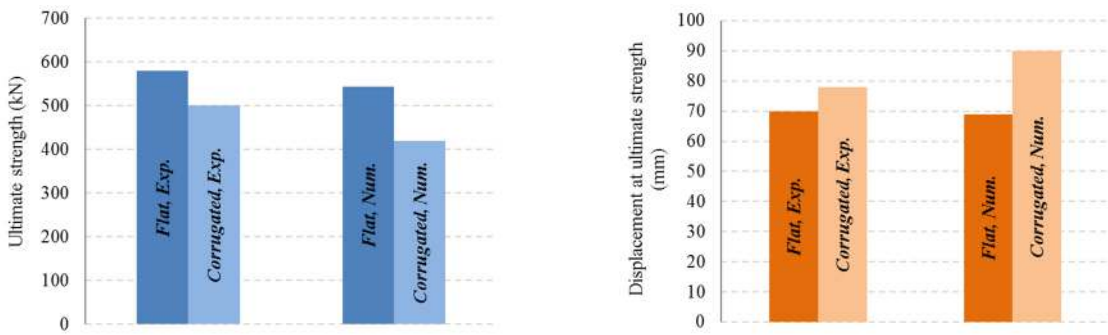

(a) (b)

Figure 6: Comparison of experimental results (Emami et al., 2013) and numerical predictions for: (a) ultimate strength and (b) displacement at ultimate strength.

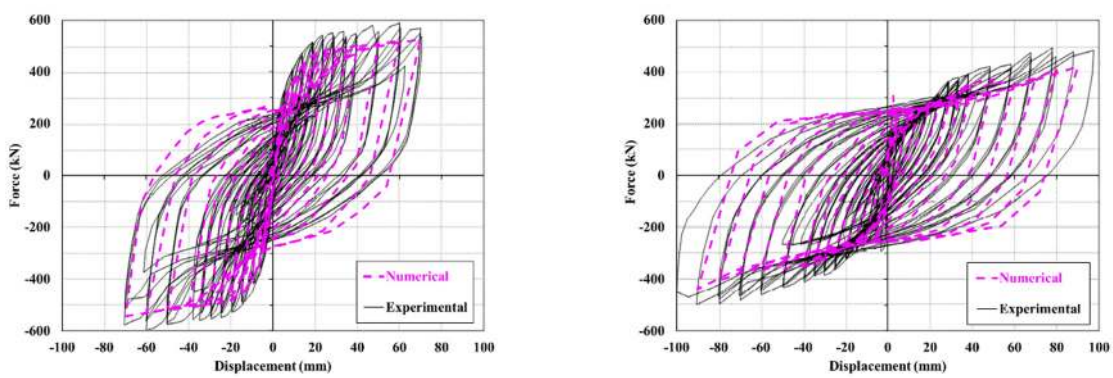

(a) (b)

Figure 7: Comparison of numericaland experimental (Emami et al., 2013) results: (a) Flat-web SPSW (b) Corrugated-web SPSW.

4 DISCUSSION OF RESULTS

4.1 Buckling Analysis

Buckling analysis was conducted to obtain the buckling modes of the flat and corrugated shear walls. It should be mentioned that elastic buckling load can be used to obtain the relative slenderness, which is a significant parameter in designing shear walls (Tong and Guo, 2015). Small out-of-plane imperfections, in accordance with the first eigen-mode, were introduced in order to allow the numerical models to trigger the deformations. The tolerated magnitudes for the mentioned trivial irregularities were a tiny proportion of the width and height of the plates. Figure 8 shows the first-buckling modes for two typical flat and corrugated models, i.e. F-1.25 and C-30-8-1.25, with respective buckling loads of 10.1kN and 336.7kN. Large amplitude lobar buckling is seen for the flat models, while horizontal buckling ripples are manifested in the corrugated shear wall, which is believed to be affected by the geometry of the corrugations. The buckling waves developed and lined up with the sinusoidal waves, as the load increased.

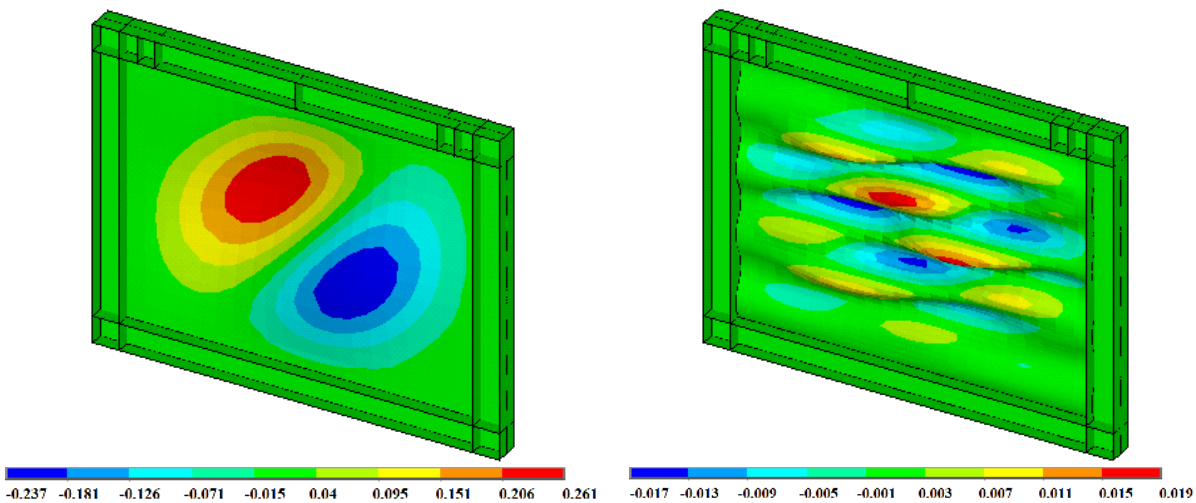

(a) *F*-1.25 (b) *C*-30-8-1.25

Figure 8: First mode of buckling.

4.2 Load-Displacement Response

Out-of-plane deformation of flat and corrugated models at two different lateral displacements is depicted in Figures 9 and 10. Figure 11 shows the load-displacement response of different corrugated models. Corrugated models with the corrugation angle of 30° were quite sensitive to the thickness variation as the ultimate load enhanced by about 3.8 times when the thickness of 1.25 mm increased up to 6 mm (see Figure 11a). The other salient point is that for thinner shear walls a bifurcation type of buckling was identified, whereas the thicker plates experienced a limit state failure against lateral loading. It should be noted that for the former models, the drop of the load was followed at the bifurcation point by a significant strain hardening, leading to a peak load in the

plastic region, while a relatively moderate nonlinearity followed by a plastic behavior were obtained for the thicker walls.

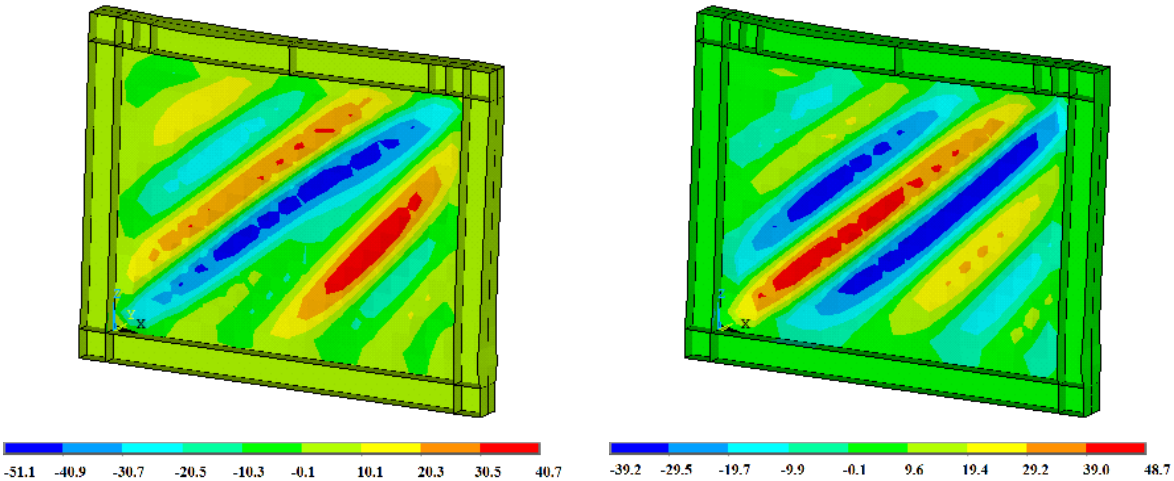

(a) lateral displacement of 60 mm (b) lateral displacement of 70 mm

Figure 9: Out-of-plane deformation for *F*-1.25.

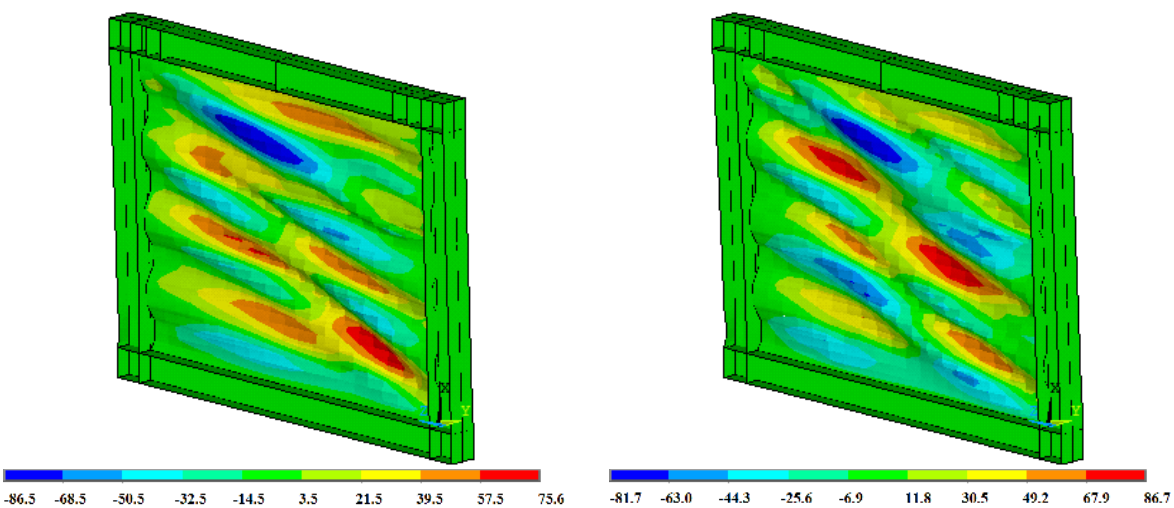

(a) lateral displacement of 60 mm (b) lateral displacement of 80 mm

Figure 10: Out-of-plane deformation for *C*-30-8-1.25.

Figure 11b shows different corrugated models, wherein the thickness of the models is 6 mm, but the number and angle of corrugation are different from one another. It appears that relatively thicker corrugated shear walls behaved similarly as a typical elastic-plastic response was observed for all of the mentioned models. Only *C*-30-8-6 behaved more unstably in the plastic region relative to the other counterparts which can be only attributed to the lower corrugation angle of this model.

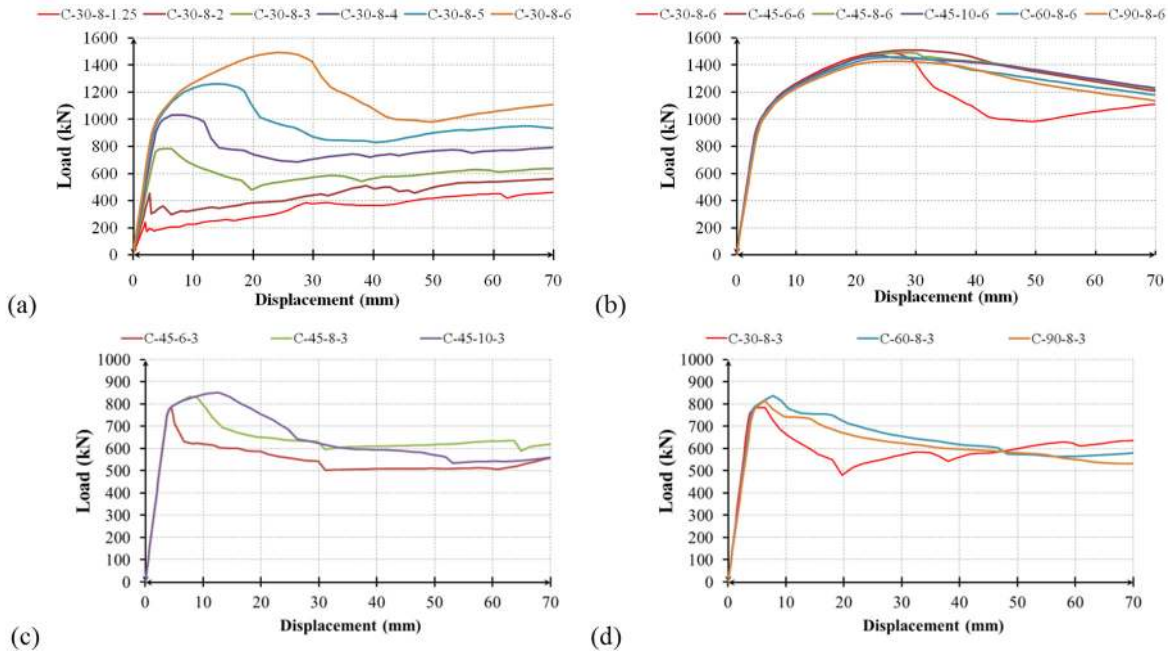

Figure 11: Load-displacement response of different models.

Figure 11c shows different models with the same thickness and corrugation angle, but different number of corrugations (*C*-45-6-3, *C*-45-8-3 and *C*-45-10-3). Bifurcation instability is seen for the model *C*-45-6-3, while the other two reached a limit state instability. Three different models with a varying corrugation angle are shown in Fig. 11d. This figure demonstrates that a more stable, yet stranger, response was obtained for the models with the corrugation angle of 60°, which appeared to outperform compared with the other models.

4.3 Energy Dissipation for Different Corrugated Models

Energy dissipation of different SPSWs with different geometric features is shown in Figure 12. These figures clearly demonstrate the significant effect of the corrugation angle in dissipating the total energy. An ebb and flow trend is seen for the models with the same number of corrugation and wall thickness, but different angles of corrugation. This suggests that the SPSW with the angle of 60°possessed the highest energy absorption among the present models as energy dissipation grew when the corrugation angle rose up until 60°, but dropped for the SPSWs with ϑ=90°. In contrast, for the thicker models with the thickness of 6 mm, shown in Figure 12b, the SPSWs with lower corrugation angles outperformed in terms of energy absorption. Given the abovementioned points, one can readily infer the significant effect of the thickness of the SPSWs. In a nutshell though, there seem to be an interaction between the thickness and the angle of rotation. The thinner models dissipated more energy when a larger angle of corrugation was applied, while the models with rather smoother corrugation angles absorbed more energy among the thicker walls.

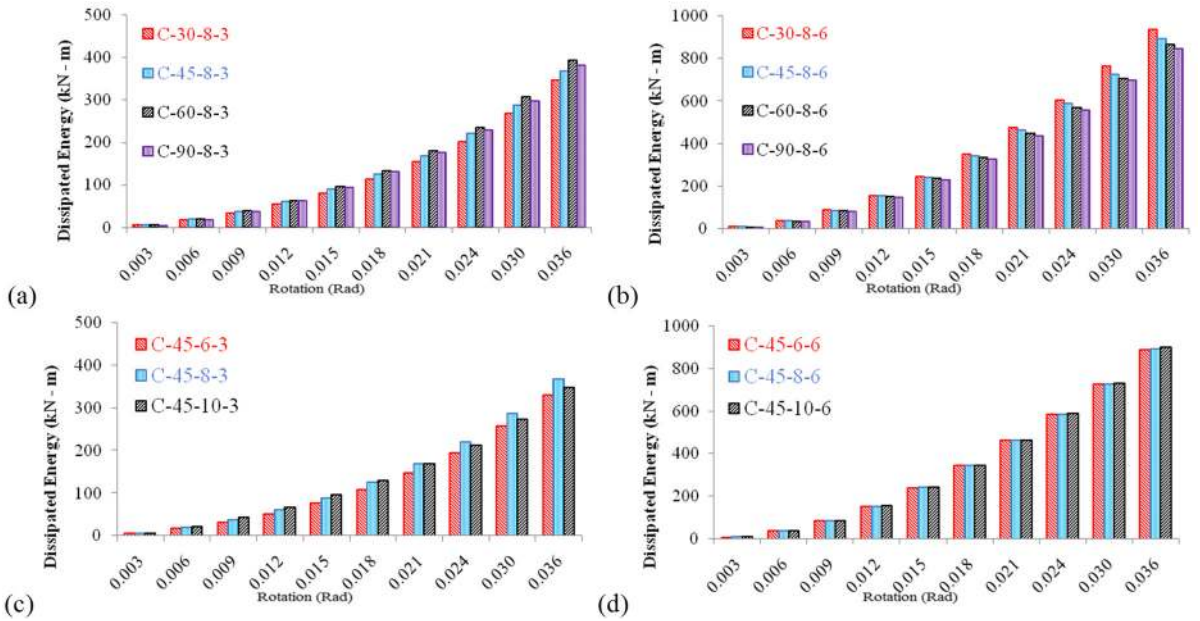

Figure 12: Dissipated energy for various models with different geometries.

Furthermore, as shown in Figure 12c, thinner models with the thickness of 3 mm, generally appeared to be more sensitive to the number of corrugations. It further appears that the models with the wall thickness of 6 mm showed quite trivial changes when the number of corrugations varied from 6 to 10, as depicted in Figure 12d.

4.4 Effect of Corrugation Angle and Number of Corrugations on the Cyclic Response

Figure 13 shows the hysteretic response of the corrugated shear walls with different angles of corrugation, but the same number of corrugation and wall thickness. Figures 13a, b display thinner SPSWs with the thickness of 3 mm, while Figures 13c, d present the hysteretic plots of the thicker walls (T=6 mm). It is plainly seen that energy dissipated more abruptly in thinner SPSWs in the first loop, while fairly gradual energy decay is clearly seen for the thicker walls. As another difference, tweaking is detected for the SPSWs with the thickness of 3 mm in the first cycles against lateral loading, whereas the first loop transitioned quite gently as the number of cycles increased for the models with the thickness of 6 mm. Figure 14 shows the hysteretic behavior of six different specimens, which were categorized and presented in two groups (T=3 and T=6 mm) to ease comparison and understanding. Note that every model in the mentioned figure has a moderate corrugation angle, i.e. 45°. It appears that the number of corrugation does not affect the cyclic response of the mentioned SPSWs as the hysteretic curves of the models with various numbers of the corrugation were smoothly aligned one over another.

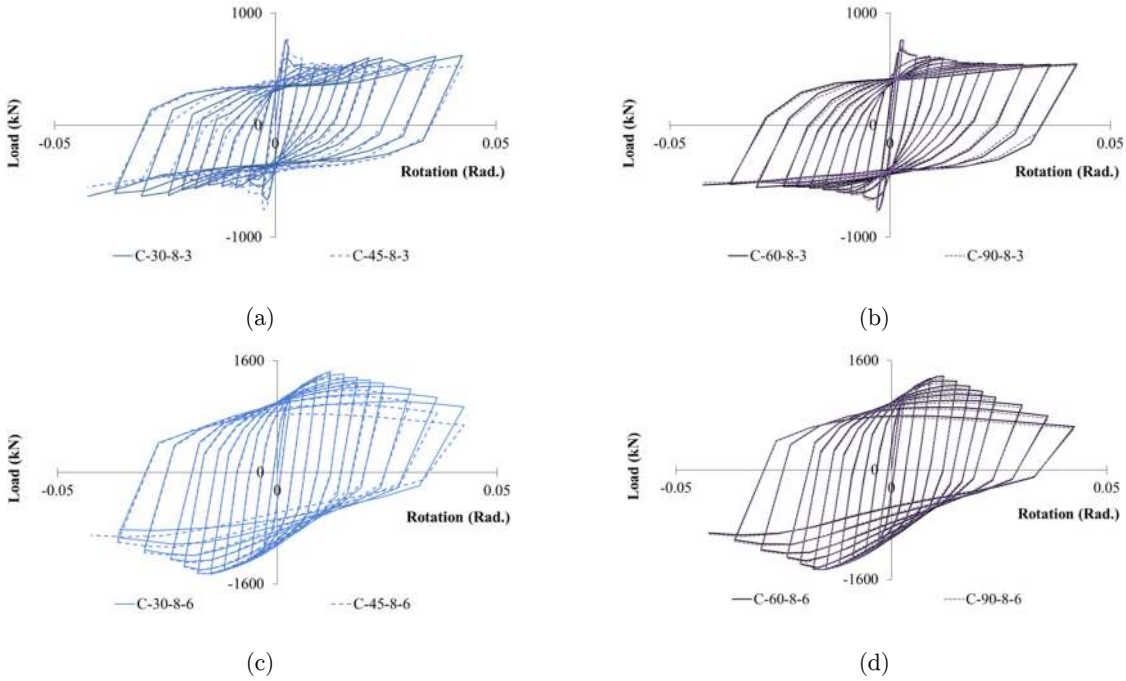

Figure 13: Effect of corrugation angle on various models with the same number of corrugation and wall thickness.

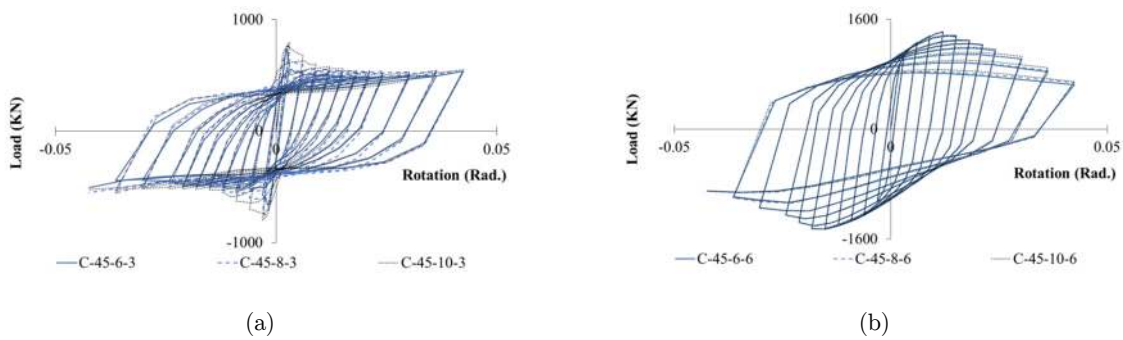

Figure 14: Variation of number of corrugations for shear walls with the same angle of corrugation and wall thickness.

5 SUMMARY AND CONCLUSIONS

Despite copious papers in the literature on the structural performance of steel shear walls, corrugated steel shear walls with sinusoidal plates were studied via detailed numerical simulations in this paper. Key findings of the research are presented in the following:

Corrugated models with the corrugation angle of 30° were quite sensitive to the thickness variation as the ultimate load enhanced by about 3.8 times when the thickness of 1.25 mm increased up to 6 mm. For thinner shear walls, a bifurcation buckling was identified, whereas the thicker plates experienced a limit state failure against lateral loading. A more stable, yet stranger, response was

obtained for the models with the corrugation angle of 60°, which appeared to outperform compared with the other models.

An ebb and flow trend of energy dissipation was seen for the models with the same number of corrugation and wall thickness, but different angles of corrugation. Notwithstanding, SPSWs with the angle of 60° possessed the highest energy absorption as energy dissipation grew when the corrugation angle rose up until 60°, but dropped for the SPSWs with ϑ=90°. The thinner models dissipated generally more energy when a larger angle of corrugation was applied, while the models with smoother corrugation angles absorbed more energy among the thicker walls. Thinner models (with the thickness of 3 mm) were predominantly more sensitive to the number of corrugations than the thicker walls.

Furthermore, energy dissipated more abruptly in thinner SPSWs in the first loop, while fairly gradual energy decay was plainly seen for the thicker walls. The number of corrugation did not affect the cyclic response of the mentioned SPSWs as the hysteretic curves of the models with various numbers of corrugations were smoothly aligned one over another.

References

ANSYS 11.0 (2007). ANSYS 11.0 Documentation, ANSYS Inc.

Emami, F., Mofid, M., Vafai, A. (2013). Experimental study on cyclic behavior of trapezoidally corrugated steel shear walls. Engineering Structures 48:750-762.

Farzampour, A., Laman, J.A. (2015). Behavior prediction of corrugated steel plate shear walls with openings. Journal of Constructional Steel Research 114:258-268.

Fülöp, L., Dubina, D. (2004a). Performance of wall-stud cold-formed shear panels under monotonic and cyclic loading: Part I: Experimental research. Thin-Walled Structures 42:321-338.

Fülöp, L., Dubina, D. (2004b). Performance of wall-stud cold-formed shear panels under monotonic and cyclic loading: Part II: Numerical modelling and performance analysis. Thin-Walled Structures 42:339-349.

Mohebbi, S., Mirghaderi, R., Farahbod, F., Sabbagh, A.B. (2015). Experimental work on single and double-sided steel sheathed cold-formed steel shear walls for seismic actions. Thin-Walled Structures 91:50-62.

Purba, R., Bruneau, M. (2015). Experimental investigation of steel plate shear walls with in-span plastification along horizontal boundary elements. Engineering Structures 97:68-79.

Sabouri-Ghomi, S., Mamazizi, S. (2015). Experimental investigation on stiffened steel plate shear walls with two rectangular openings. Thin-Walled Structures 86:56-66.

Stojadinovic, B., Tipping, S. (2007).Structural testing of corrugated sheet steel shear walls. Research report, University of California, Berkeley.

Tian, H.W., Li, Y.Q., Yu, C. (2015). Testing of steel sheathed cold-formed steel trussed shear walls. Thin-Walled Structures 94:280-292.

Tong, J.Z., Guo, Y.L. (2015). Elastic buckling behavior of steel trapezoidal corrugated shear walls with vertical stiffeners. Thin-Walled Structures 95:31-39.

Vigh, L.G., Deierlein, G.G., Miranda, E., Liel, A.B., Tipping, S. (2013). Seismic performance assessment of steel corrugated shear wall system using non-linear analysis. Journal of Constructional Steel Research 85:48-59.

Vigh, L.G., Liel, A.B., Deierlein, G.G., Miranda, E., Tipping, S.(2014). Component model calibration for cyclic behavior of a corrugated shear wall. Thin-Walled Structures 75:53-62.

Vora,H., Yu, C. (2008). Pilot research on cold-formed steel framed shear wall assemblies with corrugated sheet steel sheathing. Proceedings of the19thInternational specialty conference on cold-formed steel structures, St. Louis, 14-15.

Wang, X., Ye, J. (2015). Reversed cyclic performance of cold-formed steel shear walls with reinforced end studs. Journal of Constructional Steel Research 113:28-42.

Zhang, J., Zirakian, T. (2015). Probabilistic assessment of structures with SPSW systems and LYP steel infill plates using fragility function method. Engineering Structures 85:195-205.

Zirakian, T., Zhang, J. (2015). Buckling and yielding behavior of unstiffened slender, moderate, and stocky low yield point steel plates. Thin-Walled Structures 88:105-118.